AIAA 80-0766R

Design for Active Flutter Suppression and Gust Alleviation Using State-Space Aeroelastic Modeling

Mordechay Karpel*
Stanford University, Stanford, Calif.

An analytical design technique for an active flutter-suppression and gust-alleviation control system is presented. It is based on a rational approximation of the unsteady aerodynamic loads in the entire Laplace domain, which yields matrix equations of motion with constant coefficients. Some existing rational approximation schemes are reviewed, and a new technique which yields a minimal number of augmented states for a desired accuracy is presented. The state-space aeroelastic model is used to design a constant gain, partial-feedback control system, which simultaneously assures stability and optimizes any desired combination of gust response parameters throughout the entire flight envelope.

Nomenclature

a, b, c = geometric properties of a typical section (Fig. 1)
b_g = control command participation in z_d
C_{l_α} = lift coefficient derivative with respect to angle of attack $= L_\alpha / 2bq$
$C(\bar{s})$ = generalized Theodorsen function [Eq. (3)]
$D_0(s)$ = open-loop characteristic polynomial
h = plunge coordinate (Fig. 1)
k = reduced frequency $= \omega b / V$
$K_n(\bar{s})$ = modified Bessel function of order n
L = lift per unit span
L_g = scale of turbulence, length units
m = order of the denominator polynomial in a rational approximation
m_c = number of output measurements
m_s = wing mass per unit span
M = Mach number
M_α, M_β = pitching and hinge moments (Fig. 1)
n = number of degrees of freedom
n_c = order of Eq. (17)
q = dynamic pressure $= \frac{1}{2}\rho V^2$
r = magnitude of $\bar{s} = re^{i\theta}$
r_α^2, r_β^2 = radius of gyration of the typical section and the control surface, divided by b
s = Laplace transform variable
$\bar{s}$ = nondimensionalized Laplace variable $= sb/V$
$u, U(s)$ = control command variable and its Laplace transform
V = airspeed
w_g = vertical gust velocity
x_α, x_β = dimensionless center of mass offsets (Fig. 1)
$z_d, Z_d(s)$ = gust response design variable and its Laplace transform
α = angle of attack
β, β_c = control surface actual and command rotations
γ_j = aerodynamic roots [Eq. (5)]
ϵ = error of least-square approximation
$\Phi_{w_g}(\omega)$ = power spectral density of w_g
λ = wavelength of sinusoidal gust
μ = mass ratio $= m_s / \pi\rho b^2$
ρ = air density
$\sigma_{w_g}^2$ = mean square value of w_g
θ = argument of $\bar{s}$
ω = vibration frequency, rad/s
$\omega_h, \omega_\alpha, \omega_\beta$ = plunge, pitch, and flap uncoupled natural frequencies

Matrices

adj [ ] = adjoint matrix of [ ]
$[A]$ = aerodynamic influence coefficients
$[A_{ap}]$ = approximated value of $[A]$
$[a_g]$ = states participating in z_d
$\{A_g\}$ = gust loads influence coefficients
$[A_{j,l}], [B_{j,l}]$ = as defined in Eq. (9)
$[B]$ = damping matrix
$[C]$ = control gains
$[C(\bar{R}, k_l)]$ = as defined in Eq. (15)
$[D], [\bar{D}]$ = defined in Eqs. (11) and (13)
$[E], [\bar{E}]$ = defined in Eqs. (11) and (13)
$[F(k)], [G(k)]$ = real and imaginary parts of $[A(ik)]$
$[F_l], \{G_l\}$ = dynamic and input matrices of Eq. (17)
$\{g(s)\}$ = as defined in Eq. (21)
$[H], \{J\}$ = output matrices of Eq. (17)
$[I]$ = unit matrix
$[K], [M]$ = stiffness and mass matrices
$[P_i]$ = coefficients of matrix polynomial
$[Q_{pl}]$ = piston theory limit, $[G(k)]/k, k \to \infty$
$[R], [\bar{R}]$ = defined in Eqs. (12) and (13)
$\{R_l\}, [S_1], [S_2]$ = define the circulatory parts of Eq. (2)
$\{x\}, \{X(s)\}$ = deflections in generalized coordinates and their Laplace transform
$\{y\}, \{Y(s)\}$ = measurement vector and its Laplace transform
$\{z\}, \{Z(s)\}$ = state vector and its Laplace transform

Subscripts

a = aerodynamic
$f, f1, f2$ = l values at which approximated and tabulated terms match
l = index of tabulated data
nc = noncirculatory aerodynamic
$r1, r2$ = reference values of l in the least-square equations
s = structural

Presented as Paper 80-0766 at the AIAA/ASME/ASCE/AHS 21st Structures, Structural Dynamics and Materials Conference, Seattle, Wash., May 12-14, 1980; submitted June 4, 1980; revision received July 16, 1981.

*Research Assistant, Department of Aeronautics and Astronautics.

Introduction

IN recent years, extensive research has been carried out to develop active flutter suppression and gust alleviation systems, in which aerodynamic control surfaces are operated according to a control law which relates the motion of the controls to some measurements taken on the vehicle. The aerodynamic forces generated by the controls modify the overall forces in such a way as to suppress flutter and alleviate structural turbulence response within the aircraft flight envelope (including safety margins). Some recent analytical developments, wind-tunnel tests, and flight-test demonstrations[1-5] show the potential and feasibility of active aeroelastic control systems. However, in order to apply modern control techniques efficiently for optimized systems, more refined aeroelastic modeling has to be carried out.

The main difficulty in modeling an aeroelastic system for control design lies in the representation of the unsteady aerodynamic loads. The classical approach to flutter[6] is based on aerodynamic influence coefficient matrices computed for simple harmonic motion at discrete values of reduced frequencies. The flutter analysis is performed for many Mach numbers, reduced frequencies, and air densities to find the "matched" stability boundary. Only there is the assumption of simple harmonic motion correct. Nissim's energy concept[7] for flutter suppression system design is based on the same approach. Nissim's formulation was successfully used for developing some experimental systems.[2,8] Modern control analysis, however, which calls for the representation of the aerodynamic loads in the entire Laplace domain (s plane), is not suitable for Nissim's formulation. Recent developments in the evaluation of unsteady aerodynamic loads due to arbitrary motion[9] followed earlier attempts[21] and opened the way for calculating aerodynamic influence coefficients in the entire s plane. The resulting expressions are usually nonrational, however, and require lengthy calculations. In order to obtain an aeroelastic system with a finite-order state-form matrix equation for linear stability analysis, the aerodynamic influence coefficients have to be approximated by rational functions of s (namely, fraction of polynomials of s).

Rational approximations of the unsteady loads on a typical section in incompressible flow were derived by R.T. Jones[10] in a way that could be later applied to modern control theory.[14] The two roots placed by Jones along the negative real axis of the s plane idealize the time delays inherent in unsteady aerodynamic loading. Systematic techniques which use oscillatory aerodynamic matrices (along the imaginary axis of the s plane) to generate rational approximate solutions for arbitrary motion were developed by several authors.[1,9,11,12] They are reviewed in this paper, and a new technique, which minimizes the number of augmented states for a desired accuracy, is presented.

Once a suitable approximation for the aerodynamic loads is chosen, a state-space matrix equation of motion can be constructed. Since the aerodynamic loads are a function of the flow conditions, each point in the flight envelope has a different equation of motion. A root-loci analysis yields the variation of the systems frequencies of oscillation and damping ratios with the dynamic pressure for a given Mach number. After adding to the state-form equation a control (input) term and a measurement (output) equation, control analysis is performed.

There is no all-purpose control technique. A suitable one is chosen in accordance with the performance requirements, the available control means, the precision of the mathematical model, the measurement accuracy, and the on-board computer capacity. The control analysis given in this paper is for a simple constant gain, partial-feedback, single-input, continuous control system. A procedure, which simultaneously assures stability and minimizes an arbitrary gust response design parameter over the entire flight envelope, is presented. More detailed theoretical developments and numerical examples for aeroelastic modeling and control analysis are given in Ref. 20.

Unsteady Aerodynamic Modeling

The Laplace transform of the n-degree-of-freedom, open-loop, aeroelastic system equations of motion (for stability analysis) reads

$$([M_s]s^2+[B_s]s+[K_s])\{X(s)\}=q[A]\{X(s)\} \tag{1}$$

Modal coordinates are used, and s is the Laplace variable. For given geometry, mode shapes, and Mach number, the complex aerodynamic influence coefficient matrix $[A]$ is a function of $\bar{s}=sb/V$.

A fundamental phenomenon in unsteady subsonic aerodynamics is that the disturbances shed into the flow by the wing motion continue to affect the loads at a later time. Mathematically this phenomenon results in nonrational expressions for the aerodynamic influence coefficients; they usually cannot be exactly represented in the Laplace domain by transfer functions of finite order. In order to solve Eq. (1) by the methods of linear algebra, $[A]$ has to be approximated by rational functions of $\bar{s}$.

Incompressible, Two-Dimensional Flow

The unsteady aerodynamic loads on the typical section of Fig. 1, in incompressible, two-dimensional flow, were formulated by Theodorsen[13] for oscillatory motion. Following Sears,[15] and Luke and Dengler,[21] Edwards[14] showed that these results may be generalized for arbitrary motion. The influence coefficient matrix is

$$[A]=[M_{nc}]\bar{s}^2+[[B_{nc}]+C(\bar{s})\{R_1\}[S_2]]\bar{s}$$
$$+[K_{nc}]+C(\bar{s})\{R_1\}[S_1] \tag{2}$$

where $C(\bar{s})$ is the generalized Theodorsen function

$$C(\bar{s})=K_1(\bar{s})/(K_0(\bar{s})+K_1(\bar{s})) \tag{3}$$

where K_n is a modified Bessel function of order n. $C(\bar{s})$ is analytic throughout the $\bar{s}$ plane except for a branch point at the origin, which requires a branch cut along the negative real axis. The other terms in Eq. (2) are given in Ref. 14.

Rational fraction approximation of the generalized Theodorsen function derives from the R.T. Jones[10] approximation of Wagner's indicial loading function as

$$C(\bar{s})\simeq 0.5+\frac{0.0075}{\bar{s}+0.0455}+\frac{0.10055}{\bar{s}+0.3} \tag{4}$$

Padé Approximants

Unlike the incompressible, two-dimensional aerodynamics [Eq. (2)], in a more general aeroelastic system there is no longer a single nonrational function which can be factored out of the influence coefficient matrices. This led to a Padé ap-

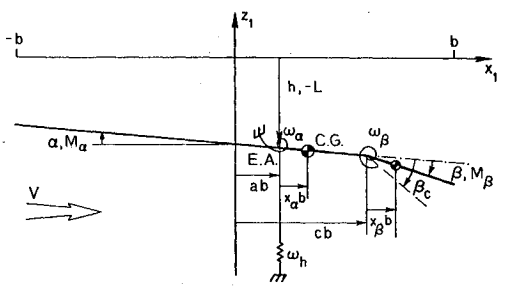

Fig. 1 A typical-section flutter model, showing definitions of coordinates and system properties.

proximant technique[1,12] in which each term of the influence coefficient matrix is approximated by a different ratio of polynomials in s.

In a Padé approximant of order m, a least-square technique is used to find the numerator and denominator polynomials which best fit tabulated influence coefficients for oscillatory motion. Since each approximation root adds one state to the equation of motion, the dimension of an n-degree-of-freedom model becomes $2n+mn^2$. In a realistic problem, the contributions of some of these roots are negligible and are omitted. In the design problem of Ref. 1, for instance, a system of 27 structural modes was analyzed with a mathematical model of order 200.

Roger's Approximation

Roger[11] realized that the aerodynamic influence coefficients may be approximated more efficiently by using common denominator roots. Roger's approximation is

$$[A_{ap}] = [P_0] + [P_1]\bar{s} + [P_2]\bar{s}^2 + \sum_{j=3}^{N} \frac{[P_j]\bar{s}}{(\bar{s}+\gamma_{j-2})} \tag{5}$$

where the values of γ_{j-2} are selected to be in the reduced frequency range of interest. The real coefficient matrices $[P]$ are found by setting $\bar{s}=ik$ and using a least-square technique for a term-by-term fitting of tabulated oscillatory influence coefficient matrices.

Roger's approximation yields a model of order Nn. Most applications (such as Refs. 5 and 8) used $N=6$.

Matrix Padé Approximation

The matrix Padé approximant technique was introduced by Vepa,[12] modified by Edwards,[9] and is further modified here. The approximant is

$$[A_{ap}] = (\bar{s}[I] - [R])^{-1}([P_1]\bar{s}^2 + [P_2]\bar{s} + [P_3]) \tag{6}$$

The data used to determine the approximant consists of tabulated steady-state influence coefficients $[F(0)]$ and oscillatory influence coefficients $[A(ik_l)] = [F(k_l)] + i[G(k_l)]$ for various l indices. A requirement of matching the steady-state aerodynamics yields

$$[P_3] = -[R][F(0)] \tag{7}$$

$[P_1]$ and $[P_2]$ are related to $[R]$ by

$$[P_1] = [R]\{[F(k_{f1})] - [F(0)]\}/k_{f1}^2 + [G(k_{f1})]/k_{f1} \tag{8a}$$

and

$$[P_2] = [F(k_{f2})] - [R][G(k_{f2})]/k_{f2} \tag{8b}$$

where k_{f1} and k_{f2} are selected from the tabulated k values. Equations (8a) and (8b) are only approximations at other k_l values, for which

$$[A_{1,l}]^T[R]^T \simeq [B_{1,l}]^T \tag{9a}$$

and

$$[A_{2,l}]^T[R]^T \simeq [B_{2,l}]^T \tag{9b}$$

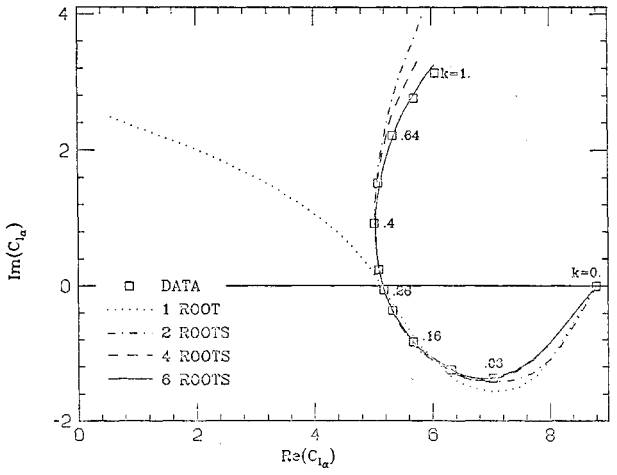

Fig. 3 Minimum state approximants of C_{l_α} for a typical section at $M=0.7$ as a function of $\bar{s}=ik$.

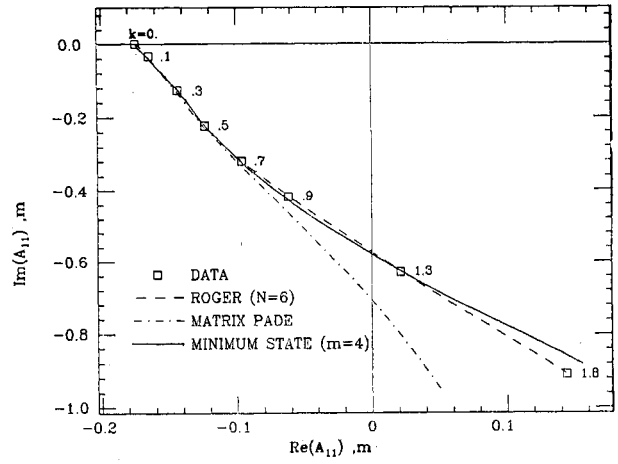

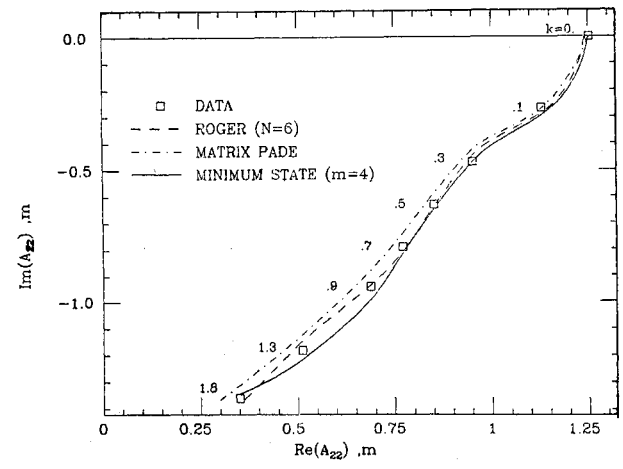

Fig. 4 Curve fitting for A_{11} and A_{22} of rational approximations to aerodynamic influence coefficients of the Ref. 5 wing at $M=0.9$.

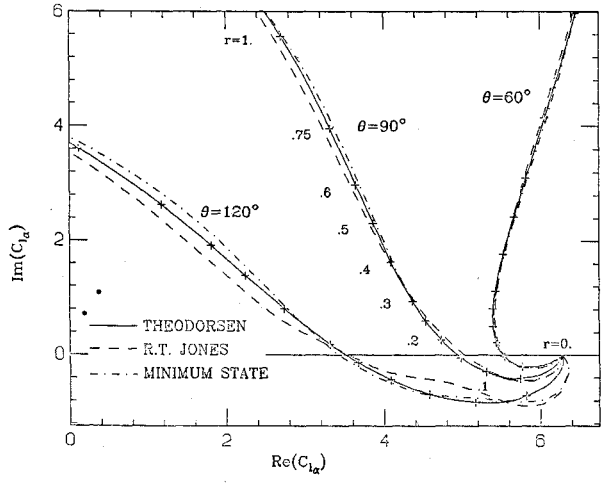

Fig. 2 R.T. Jones and minimum state approximations for C_{l_α} of a typical section in incompressible flow as a function of $\bar{s}=re^{i\theta}$.

where

$$[A_{1,l}] = \{[F(k_l)] - [F(0)]\}/k_l^2 - \{[F(k_{rl})] - [F(0)]\}/k_{rl}^2$$

$$[A_{2,l}] = [G(k_l)]/k_l - [G(k_{r2})]/k_{r2}$$

$$[B_{1,l}] = [G(k_{rl})]/k_{rl} - [G(k_l)]/k_l$$

and

$$[B_{2,l}] = [F(k_l)] - [F(k_{r2})]$$

where k_{rl} and k_{r2} are selected from the k_l values.

Edwards[9] used $k_{f1} = k_{f2} = k_f$, which causes the approximant to be exact at k_f. He chose $k_{rl} \to \infty$, which yields $\{[F(k_{rl})] - [F(0)]\}/k_{rl}^2 \to 0$ and $[G(k_{rl})]/k_{rl} \to [Q_{pl}]$. He also used Eq. (9a) only to construct a matrix least-square problem to be solved for $[R]^T$.

The matrix Padé approximation is improved when both Eqs. (9a) and (9b) are used for least-square fitting, which yields

$$\left[\sum_l \sum_{j=1}^{2} [A_{j,l}][A_{j,l}]^T\right][R]^T = \sum_l \sum_{j=1}^{2} [A_{j,l}][B_{j,l}]^T \tag{10}$$

Best overall accuracy is obtained by taking $k_{f1} = k_{rl} = \max(k_l)$ and $k_{f2} = k_{r2} = k_l$ at which accuracy is most important. The matrix Padé technique yields a state-space model[9] of order $3n$.

The Minimum-State Method

The most general representation of an open-loop aeroelastic system by a finite state-space equation of motion can be written as

$$\begin{Bmatrix} \dot{x} \\ \ddot{x} \\ \dot{x}_a \end{Bmatrix} = \begin{bmatrix} 0 & [I] & 0 \\ -[M_s+M_a]^{-1}[K_s+K_a] & -[M_s+M_a]^{-1}[B_s+B_a] & [M_s+M_a]^{-1}[D] \\ 0 & [E] & [R] \end{bmatrix} \begin{Bmatrix} x \\ \dot{x} \\ x_a \end{Bmatrix} \tag{11}$$

where $\{x\}$ is the generalized coordinate vector of an n-degree-of-freedom system and $\{x_a\}$ is a vector of m augmented states. Comparing Eq. (11) with Eq. (1) shows that the aerodynamic influence coefficient matrix is approximated by

$$[A_{ap}(\bar{s})] = [P_1]\bar{s}^2 + [P_2]\bar{s} + [P_3] + [\bar{D}](\bar{s}[I] - [\bar{R}])^{-1}[\bar{E}]\bar{s} \tag{12}$$

(dimensions: $[A_{ap}(\bar{s})]$ nxn; $[P_1]$, $[P_2]$, $[P_3]$ nxn; $[\bar{D}]$ nxm; $(\bar{s}[I] - [\bar{R}])$ mxm; $[\bar{E}]$ mxn)

where the aerodynamic parameters of Eq. (11) are related to those of Eq. (12) by

$$[M_a] = -\tfrac{1}{2}\rho b^2[P_1], \quad [B_a] = -\tfrac{1}{2}\rho bV[P_2]$$

$$[K_a] = -\tfrac{1}{2}\rho V^2[P_3], \quad [D] = \tfrac{1}{2}\rho V^2[\bar{D}] \tag{13}$$

$$[E] = [\bar{E}], \quad [R] = (V/b)[\bar{R}], \quad s = \bar{s}V/b$$

The approximation of Eq. (12) is constrained to match the influence coefficients for $k = 0$ and $k = k_f$, which yields

$$[P_1] = \{[F(0)] - [F(k_f)]\}/k_f^2 + [\bar{D}](k_f^2[I] + [\bar{R}]^2)^{-1}[\bar{E}] \tag{14a}$$

$$[P_2] = [G(k_f)]/k_f + [\bar{D}](k_f^2[I] + [\bar{R}]^2)^{-1}[\bar{R}][\bar{E}] \tag{14b}$$

$$[P_3] = [F(0)] \tag{14c}$$

For the other tabulated reduced frequencies, Eqs. (14a) and (14b) become approximations. Thus one obtains

$$[\bar{D}][C(\bar{R},k_l)][\bar{E}] \simeq \{[F(k_l)] - [F(0)]\}/k_l^2 - \{[F(k_f)] - [F(0)]\}/k_f^2 \tag{15a}$$

and

$$[\bar{D}][C(\bar{R},k_l)][\bar{R}][\bar{E}] \simeq [G(k_f)]/k_f - [G(k_l)]/k_l \tag{15b}$$

where

$$[C(\bar{R},k_l)] = (k_l^2[I] + [\bar{R}]^2)^{-1} - (k_f^2[I] + [\bar{R}]^2)^{-1}$$

For a given approximation, order m, the problem is to find the matrices $[\bar{D}]$, $[\bar{E}]$, and $[\bar{R}]$ which best fit the tabulated data at several k_l values. Since the eigenvalues of $[\bar{R}]$ represent the time delay in the aerodynamic loads, $[\bar{R}]$ is chosen to be diagonal with negative elements.

The minimum-state procedure goes as follows: 1) Set an initial number of augmented states m; 2) set an initial diagonal $[\bar{R}]$ with distinct negative elements; 3) set an initial $[\bar{D}]$ with rank $[\bar{D}] = \min(m,n)$; 4) use Eqs. (15a) and (15b) to set and solve a matrix least-square problem for $[\bar{E}]$ [cf. Eq. (10)]; 5) use Eqs. (15a) and (15b) (transposed) to set and solve a matrix least-square problem for $[\bar{D}]$; 6) calculate the least-square performance index ($\Sigma\epsilon^2$); 7) repeat steps 4-6 to convergence; 8) use a minimization procedure to modify $[\bar{R}]$; 9) repeat steps 3-8 until the performance index converges to a global minimum; 10) calculate the approximant of Eq. (12) for the tabulated reduced frequencies and compare with the tabulated data; 11) if the accuracy of the approximant is not satisfactory, increase m and repeat steps 2-10.

We can see from Eq. (15) that the least-square problem actually approximates $\{[F(k_l)] - [F(0)]\}/k_l^2$ and $[G(k_l)]/k_l$. The low frequency coefficients are weighted more than the high frequency ones. Other means for controlling the variation of the accuracy with k are selection of data points and of the value of k_f.

While the weighting of Eq. (15) is suitable for incompressible flow, different weighting can be used in other cases. With uniform weighting Eq. (15) becomes

$$k_l^2[\bar{D}][C(\bar{R},k_l)][\bar{E}] \simeq [F(k_l)] - [F(0)] - \{[F(k_f)] - [F(0)]\}(k_l/k_f)^2 \tag{16a}$$

and

$$k_l[\bar{D}][C(\bar{R},k_l)][\bar{R}][\bar{E}] \simeq [G(k_f)]k_l/k_f - [G(k_l)] \tag{16b}$$

Numerical Examples Employing Rational Approximants

The minimum-state procedure is first applied to the typical section of Fig. 1 in incompressible flow with $a = -0.4$, $b = 1$, and $c = 0.6$. The tabulated aerodynamic influence coefficients were calculated for $k = 0$, $k_f = 0.25$, and $k_l = 0.1$, 0.15, 0.2, 0.3, 0.5, 1, and 2 from Theodorsen's version of Eq. (2). The least-square approximation is that of Eq. (15). A comparison between C_{l_α} obtained from Theodorsen (as generalized in Refs. 14 and 21), the R.T. Jones approximation [Eq. (4)], and the minimum-state method of order 2 [Eq. (12)], is given in Fig. 2 for various values of $\bar{s} = re^{i\theta}$.

The minimum-state procedure is seen to yield a better approximation in the entire range of interest $|r| < 1$, and

60 deg $< \theta <$ 120 deg. Both approximations deteriorate as the branch cut along the negative real axis is approached.

The minimum-state procedure, with the least-square approximation of Eq. (15), was also applied to a typical section in subsonic flow of $M=0.7$. The tabulated aerodynamic matrices for $k=0$, $k_f=0.26$, and $k_l=0.06$, 0.1, 0.16, 0.22, 0.3, 0.4, 0.5, 0.64, 0.8, and 1.0 were taken from Ref. 16. The approximants of order 1, 2, 4, and 6 are compared to the tabulated oscillatory C_{l_α} in Fig. 3. The first-order approximation is quite poor. Starting with $m=2$, it is up to the designer to make the tradeoff between the approximation accuracy and the order of the resulting model.

The last example chosen was a model wing used for demonstration of active flutter suppression in the wind tunnel. The wing characteristics and a stability analysis are given by Abel.[5] Abel used Roger's approximation [Eq. (5)], with $N=6$. Oscillatory aerodynamic influence coefficients for $M=0.9$ were calculated for $k=0$, 0.1, 0.3, 0.5, 0.7, 0.9, 1.3, and 1.8, using the doublet-lattice aerodynamics.[22] The values of γ_{j-2} in Eq. (5) are 0.2, 0.4, 0.6, and 0.8.

The minimum-state technique, with no k weighting [Eq. (16)] and with $k_f=0.3$, was applied to a system consisting of four vibration modes. Three wing modes (1,2, and 4),[5] which affect the flutter mechanism, and the control surface deflection mode were selected and normalized for unit generalized masses. The modified matrix Padé technique was also applied (with the wing modes only), and best results were obtained with $k_{f1}=k_{r1}=1.8$ and $k_{f2}=k_{r2}=0.3$.

Curve fittings for A_{11} and A_{22} using Roger's approximation, the modified matrix Padé approximant, and the minimum-state approximation of order 4 are shown in Fig. 4. The minimum-state fit (with four augmented states) is comparable with Roger's fit based on 16 augmented states. The matrix Padé fit is much less accurate than the other two.

Control Analysis

The purpose of this section is to demonstrate the usage of a state-space representation of an aeroelastic system in flutter suppression and gust alleviation. The focus is on optimizing a predetermined partial feedback control law over a wide range of aerodynamic parameters. The control equations and the numerical example are deliberately simple. More general control analysis and more practical numerical examples are dealt with in Ref. 20.

The open-loop equation of motion (11) is now supplemented with a single-input term and a multi-output (measurement) equation. The control equations are

$$\begin{aligned} &\underset{n_c x 1}{\{\dot{z}\}} = [F_l]\{z\} + \{G_l\}u, \qquad n_c = 2n+m \\ &\underset{m_c x 1}{\{y\}} = [H]\{z\} + \{J\}u, \qquad m_c \le n_c \end{aligned} \tag{17}$$

Here $\{z\}$ and $[F_l]$ are the state vector and the dynamic matrix of Eq. (11), u is the control variable and $\{y\}$ is the measurement vector. It is assumed that the generalized forces, generated by u, are proportional to the control command. More complicated dynamics of the actuator system can be modeled by additional states or compensated for in the final control law.[5] The actual control surface motion states are part of $\{z\}$. $[F_l]$, $\{G_l\}$, $[H]$, and $\{J\}$ may vary with Mach number and dynamic pressure.

The design target in this paper is for a constant coefficient control law

$$u = [C]\{y\} \tag{18}$$

which suppresses flutter in the entire flight envelope and yields minimal mean square response of a selected design parameter.

Pole Assignment

The Laplace transform of Eq. (17) yields the input-output transfer function

$$\frac{\{Y(s)\}}{U(s)} = [H](s[I]-[F_l])^{-1}\{G_l\} + \{J\} \tag{19}$$

Substituting the Laplace transform of Eq. (18) for $U(s)$ and premultiplying Eq. (19) by $[C]$ yields

$$[C]\{[H](s[I]-[F_l])^{-1}\{G_l\} + \{J\}\} = I \tag{20}$$

Using the algebraic relation

$$(s[I]-[F_l])^{-1} = \text{adj}(s[I]-[F_l]) / |s[I]-[F_l]|$$

Eq. (20) can be replaced by

$$[C](\{H\}\{g(s)\} + D_0(s)\{J\}) = D_0(s) \tag{21}$$

where

$$\{g(s)\} = \{\text{adj}(s[I]-[F_l])\}\{G_l\}, \quad D_0(s) = |s[I]-[F_l]|$$

An efficient algorithm for calculating the polynomial coefficients of $\{g(s)\}$ and $D_0(s)$ is given by Gantmakher.[17] Requiring the closed-loop system to have a specific pole at any one flight condition gives an equation (21) for the coefficients of $[C]$. A complex pole assignment gives two equations, for the real and imaginary parts of Eq. (21). A set of m_c assigned poles gives m_c equations to be solved for $[C]$. Different poles can be assigned for different flight conditions.

Once the control gains are found, the closed-loop poles at any flight condition can be found by solving the eigenvalue problem

$$\left[[F_l] + \frac{1}{1-[C]\{J\}}\{G_l\}[C][H]\right]\{Z(s)\} = s\{Z(s)\} \tag{22}$$

Gust Response Analysis

The gust response analysis is similar to that given by Pratt.[18] The response to a sinusoidal vertical gust with a unit velocity amplitude and wavelength λ is found by solving

$$\left[i\omega[I] - [F_l] - \frac{1}{1-[C]\{J\}}\{G_l\}[C][H]\right]\{Z(i\omega)\} = \{F_g\} \tag{23}$$

where

$$\{F_g\}^T = [\underset{n}{0},\ (q/V)\{A_g(ik)\}^T\underset{n}{}[M_s+M_a]^{-T},\ \underset{m}{0}]$$

and

$$\omega = 2\pi V/\lambda$$

The gust influence coefficients $\{A_g(ik)\}$ are calculated for some discrete reduced frequencies k_l and then interpolated along the imaginary axis in a way similar to the rational approximations of the previous section.

A design variable z_d is defined as a linear combination of the state variables and the control command. The frequency response of the design variable is

$$Z_d(i\omega) = \left[[a_g] + \frac{b_g}{1-[C]\{J\}}[C][H]\right]\{Z(i\omega)\} \tag{24}$$

The atmospheric turbulence is defined in statistical terms. For isotropic turbulence, the power spectral density (PSD) of the gust velocity is[6]

$$\Phi_{w_g}(\omega) = \frac{\sigma_{w_g}^2}{\pi}\frac{L_g}{V}\frac{1+3(\omega L_g/V)^2}{[1+(\omega L_g/V)^2]^2} \tag{25}$$

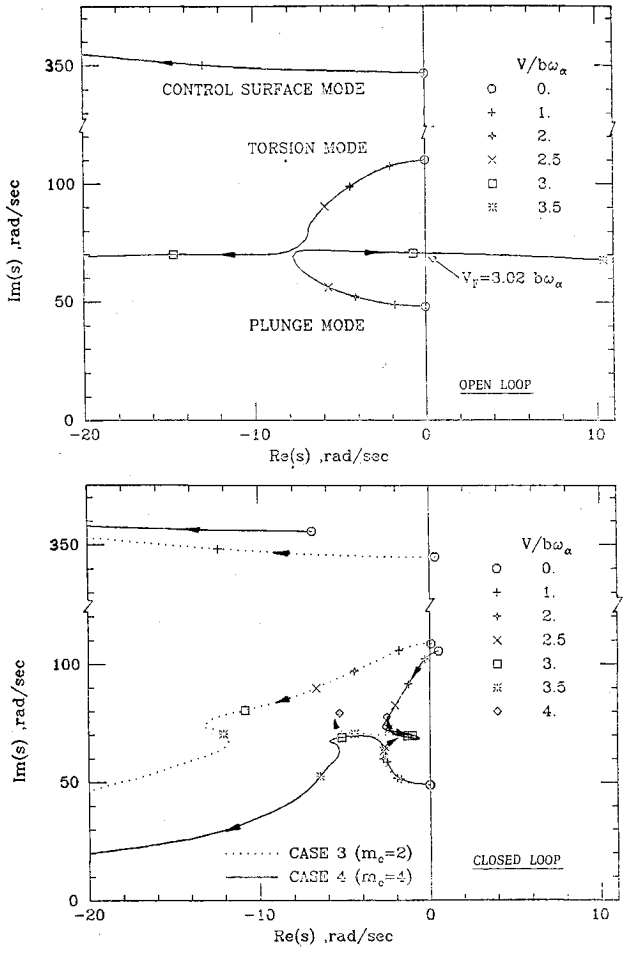

Fig. 5 Open- and closed-loop root loci for a typical section in incompressible flow.

The scale L_g depends on flight altitude and other factors. The mean square of the gust response is

$$\sigma_{z_d}^2 = \int_0^\infty |Z_d(i\omega)|^2 \Phi_{w_g}(\omega)\,d\omega \qquad (26)$$

The design cost function is some combination of $\sigma_{z_d}^2$ at several points of the flight envelope. Davidon's minimization method, as modified by Stewart,[19] is used to find the assigned poles which yield minimal cost function. The initial assigned poles must stabilize the system at the cost function points. Careful choice of these points leads to a control law, if there is any, which stabilizes the system throughout the entire flight envelope.

Control Analysis Example

Control analysis was performed for the typical section of Fig. 1 in incompressible flow. The minimum-state approximated coefficients, described in the first example of the previous section are used to model the system with six structural states and two augmented states. The structural parameters are $\omega_h = 50$ rad/s; $\omega_\alpha = 100$ rad/s; $\omega_\beta = 300$ rad/s; $\mu = 40$; $x_\alpha = 0.2$; $r_\alpha^2 = 0.25$; $x_\beta = -0.025$; $r_\beta^2 = 0.00625$. No structural damping is included.

The variables of Eq. (17) are $\{z\}^T = [h/b,\ \alpha,\ \beta,\ \dot{h}/b,\ \dot{\alpha},\ \dot{\beta},\ x_{a1},\ x_{a2}]$ and $u = \beta_c$. The open-loop ($\beta_c = 0$) root loci (Fig. 5) show a violent flutter at $V = 3.02\ b\omega_\alpha$. The control system is required to ensure no flutter between $V/b\omega_\alpha = 1$ and 3.5, and to minimize the cost function $\sigma_{z_d}^2 (V = 2.5 b\omega_\alpha) + 4\sigma_{z_d}^2 (V = 2.85 b\omega_\alpha) + \sigma_{z_d}^2 (V = 3.2 b\omega_\alpha)$ of the design variable $z_d = \dot{\beta}$. The gust influence coefficients $\{A_g(ik)\}$ were derived from Eq. (5-376) of Ref. 6. The PSD parameters in Eq. (25) are $\sigma_{w_g}^2 = 1.0\ b^2/s^2$ and $L_g = 50\ b$.

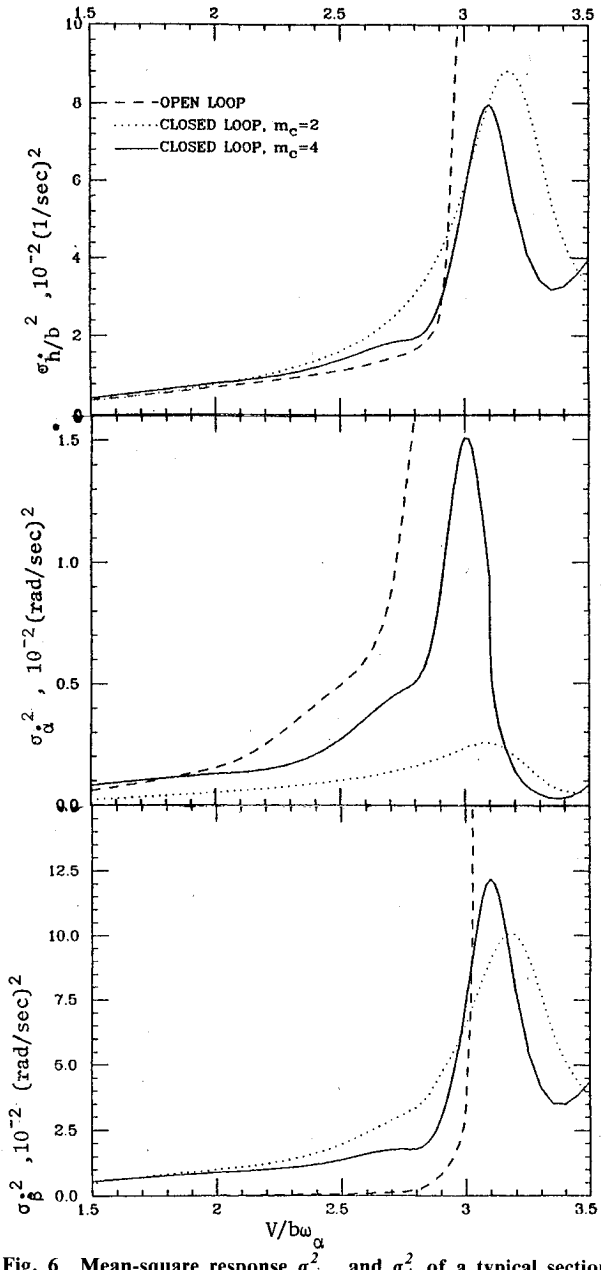

Fig. 6 Mean-square response $\sigma_{\dot{h}/b}^2$ and $\sigma_{\dot{\beta}}^2$ of a typical section in incompressible flow to atmospheric turbulence of unit mean-square velocity.

Control laws [Eq. (18)] were calculated for two cases $\{y\}^T = [h/b,\ \dot{h}/b]$ and $\{y\}^T = [h/b, \alpha,\ \dot{h}/b,\ \dot{\alpha}]$. The open-loop and closed-loop root loci are plotted in Fig. 5. The variations of $\sigma_{\dot{h}/b}^2$, $\sigma_{\dot{\alpha}}^2$, and $\sigma_{\dot{\beta}}^2$ with air speed appear in Fig. 6. We can see from the root loci that the two modes that participate in the flutter mechanism still interact with each other. But, instead of the open-loop violent bending torsion flutter, we observe a more complicated interaction which keeps the system stable. Since the measurements $\{y\}$ are of actual structural motion and the input parameter u is the commanded control surface rotation angle, the optimized control laws are physically realizable.

Figure 6 indicates that the closed-loop $\sigma_{\dot{h}/b}^2$ values are higher than the open-loop ones over a large velocity range. This is due to a more rapid increase of the closed-loop plunge frequency. It is also seen that the $\sigma_{\dot{\alpha}}^2$ graph is much higher in the four-measurements case than in the two-measurements

case. One concludes that minimizing a design gust response parameter can cause unfavorable changes in other gust response parameters.

Concluding Remarks

A new minimum-state method for efficient rational approximation of unsteady aerodynamic loads has been presented and demonstrated to result in a considerably lower-order model relative to other methods of a comparable accuracy. Because of its iterative feature the minimum-state method requires more complicated computer routines and consumes more central processor time. However, this investment pays off considerably when it comes to performing repetitive flutter and control calculations.

The minimum-state modeling technique has been used to develop state-space active control equations. A pole assignment technique, for a partial-feedback, constant-gain control law which stabilizes the system in the entire flight envelope, has been presented. The control law is modified to minimize the mean-square gust response of a design parameter over selected regions of the flight envelope.

These techniques are formulated in general form and may be applied to any flight vehicle with linearized aerodynamics. The same control equations can be used for more sophisticated optimal control techniques.

Acknowledgments

This research was done at Stanford University and was supported by NASA Research Grant NGL 05-020-243, H. Ashley, Principal Investigator. The author wishes to thank H. Ashley for his guidance and valuable suggestions during the course of this work.

References

[1] Roger, K.L., Hodges, G.E., and Felt, L., "Active Flutter Suppression—A Flight Test Demonstration," *Journal of Aircraft,* Vol. 12, June 1975, pp. 551-556.

[2] Nissim, E. and Abel, I. "Development and Application of an Optimization Procedure for Flutter Suppression Using the Energy Concept," NASA TP 1137, Feb. 1978.

[3] Hwang, C., Winther, B.A., Mills, G.R., Noll, T.E., and Farmer, M.G., "Demonstration of Aircraft Wing/Store Flutter Suppression Systems," *Journal of Aircraft,* Vol. 16, Aug. 1979, pp. 557-563.

[4] Murrow, H.N. and Eckstorm, C.V., "Drones for Aerodynamic and Structural Testing (DAST)—A Status Report," *Journal of Aircraft,* Vol. 16, Aug. 1979, pp. 521-526.

[5] Abel, I., "An Analytical Technique for Predicting the Characteristics of a Flexible Wing Equipped with an Active Flutter-Suppression System and Comparison with Wind-Tunnel Data," NASA TP 1367, 1979.

[6] Bisplinghoff, R.L., Ashley, H., and Halfman, R.L., *Aeroelasticity,* Addison-Wesley, Mass., 1955.

[7] Nissim, E., "Recent Advances in Aerodynamic Energy Concept for Flutter Suppression and Gust Alleviation Using Active Controls," NASA TN D-8519, Sept. 1977.

[8] Nissim, E. and Lottati, I., "Active Control Systems for Flutter Suppression and Gust Alleviation in Supersonic Cruise Aircraft," AIAA Paper 79-0792, April 1979.

[9] Edwards, J.H., "Applications of Laplace Transform Methods to Airfoil Motion and Stability Calculations," AIAA Paper 79-0772, April 1979.

[10] Jones, R.T., "The Unsteady Lift of a Wing of Finite Aspect Ratio," NACA Rept. 681, 1941.

[11] Roger, K.L., "Airplane Math Modeling Methods for Active Control Design," AGARD-CP-228, Aug. 1977.

[12] Vepa, R., "Finite State Modeling of Aeroelastic Systems," NASA CR-2779, 1977.

[13] Theodorsen, T., "General Theory of Aerodynamic Instability and the Mechanization of Flutter," NACA Rept. 496, 1935.

[14] Edwards, J.W., "Unsteady Aerodynamic Modeling and Active Aeroelastic Control," SUDDAR 504, Stanford Univ., Feb. 1977.

[15] Sears, W.R., "Operational Methods in the Theory of Airfoils in Nonuniform Motion," *Journal of the Franklin Institute,* Vol. 230, No. 1, July 1940.

[16] van der Vooren, A.I., "Collected Tables and Graphs," *Manual of Aeroelasticity,* Vol. IV, AGARD, Jan. 1964.

[17] Gantmakher, F.R., *Theory of Matrices,* Chelsea Pub., New York, 1959.

[18] Pratt, K.G., "Response of Flexible Airplanes to Atmospheric Turbulence," *Performance and Dynamics of Aerospace Vehicles,* NASA SP-258, 1971.

[19] Stewart, G.W., "A Modification of Davidon's Minimization Method to Accept Difference Approximations of Derivatives," *Journal of Assoc. Comput. Mach.,* Vol. 14, Jan. 1967.

[20] Karpel, M., "Design for Active and Passive Flutter Suppression and Gust Alleviation," Ph. D. dissertation, Dept. of Aeronautics and Astronautics, Stanford Univ., Aug. 1980.

[21] Luke, Y. and Dangler, M.A., "Tables of the Theodorsen Circulation Function for Generalized Motion," *Journal of the Aeronautical Sciences,* July 1951, pp. 478-483.

[22] Albano, E. and Rodden, W.P., "A Doublet-Lattice Method for Calculating Lift Distributions of Oscillating Surfaces in Subsonic Flow," *AIAA Journal,* Vol. 7, Feb. 1969, pp. 279-285.